

## ULTRA-LOW AMPLITUDE VARIABLES IN THE LMC – CLASSICAL CEPHEIDS, POP. II CEPHEIDS, RV TAU STARS AND BINARY VARIABLES

J. ROBERT BUCHLER<sup>1,2</sup>, PETER R. WOOD<sup>2</sup> & IGOR SOSZYŃSKI<sup>3</sup>

*Submitted to ApJ*

### ABSTRACT

A search for variable stars with ultra-low amplitudes (ULA), in the millimag range, has been made in the combined MACHO and OGLE data bases in the broad vicinity of the Cepheid instability strip in the HR diagram. A total of 25 singly periodic and 4 multiply periodic ULA objects has been uncovered. Our analysis does not allow us to distinguish between pulsational and ellipsoidal (binary) variability, nor between LMC and foreground objects. However, the objects are strongly clustered and appear to be associated with the pulsational instability strips of LMC Pop. I and II variables. When combined with the ULA variables of Buchler *et al.* (2005) a total of 20 objects fall close to the classical Cepheid instability strip. However, they appear to fall on parallel period-magnitude relations that are shifted to slightly higher magnitude which would confer them a different evolutionary status. Low amplitude RV Tauri and Pop. II Cepheids have been uncovered that do not appear in the MACHO or OGLE catalogs. Interestingly, a set of binaries seem to lie on a PM relation that is essentially parallel to that of the RV Tauri/Pop. II Cepheids.

*Subject headings:* stars: oscillations (including pulsations), (galaxies:) Magellanic Clouds, (stars: variables:) Cepheids, stars: variables: other, stars: Population II, instabilities, (stars:) binaries: general, (stars:) binaries (including multiple): close

### 1. INTRODUCTION

In a previous paper (Buchler *et al.* 2005), we searched for periodic variability in the light curves of selected LMC stars in MACHO Field 77. The stars were required to lie in and around the Cepheid instability strip in the HR diagram. We found seven stars with a periodic behavior of less than 0.006 mag. and labeled them ultra-low amplitude (ULA) Cepheids.

In this paper, we extend our analysis to all stars that are *common* to the OGLE II and III (Udalski et al 1999) and the MACHO (Alcock et al. 1999) data bases. The stellar selection is defined in terms of the OGLE stars that are located in a parallelogram in the HR diagram defined by  $14 < V < 17.5$  and  $18.8 < V + 9.18(V - I) < 25.0$ . This region has been chosen by visual inspection to include the instability strip and colors 0.15 blueward and redward. It contains a mixture of non-oscillatory giants of spectral type F, and variable stars such as Cepheids, W Vir stars, and ellipsoidal variables and other binaries. The region has been converted from Johnson  $V$  and Cousins  $R_c$  into MACHO blue magnitude ( $M_B$ ) and red magnitude ( $M_R$ ) using the transforms given in Alcock *et al.* (1999). Position-matched stars were examined in both the MACHO and OGLE data bases.

The standard LMC Cepheids have already been identified both in the MACHO, EROS and the OGLE data bases separately for amplitudes greater than about 0.01 mag. (Beaulieu *et al.* 1995; Welch *et al.* 1995; Udalski et al 1999; Kanbur *et al.* 2003). Our goal here is to concentrate on ULA objects.

Fourier analysis is known to be very good at detecting periodicity in data sets even in the presence of large noise. We have therefore performed a Fourier analysis of the light curves in the combined data base in the three bands MACHO  $M_R$  and  $M_B$  and OGLE I with the MUFRAN code (multi-frequency analysis, Kolláth 1990). The OGLE V band data set is generally sparse and less useful in the detection of ULA variables. The analysis is performed in the  $0 - 0.99 \text{ d}^{-1}$  frequency range, but the plotted frequency range in the subsequent figures is  $0.004 - 0.99 \text{ d}^{-1}$ , so as to avoid both the yearly and the daily aliases. One has to be careful not to miss a potential longer period that can occur in some ellipsoidals (Mennickent *et al.* 2003). We have sifted obvious outlying points from the light curves prior to analysis. In this paper all quoted amplitudes refer to Fourier amplitudes. They are determined with MUFRAN with a sinusoidal linear least-squares fit to the light curve using the frequency from the dominant Fourier peak.

We first reduce the set of over 3000 objects to those in which there are coincidences among the 8 largest Fourier peaks in  $M_R$  and OGLE I. For the standard, large amplitude Cepheids the peaks are very sharp, and these variable stars are thus readily identified. In the case of the ULA stars, the Fourier peaks  $M_R$  amplitudes fall well below 0.01 mag, but nevertheless there are coincidences among the  $M_R$  and I peaks. Each of these cases has to be examined individually to ascertain that the detected variability is not spurious. For this purpose we also use the  $M_B$  data.

We mention in passing that the typical  $M_R$ ,  $M_B$  and OGLE I window functions have a very large sharp central peak with yearly side peaks at least 45% lower, but otherwise are very dull.

We note one peculiarity with the Fourier spectra which is a result of the extremely large 1 day alias of the data:

<sup>1</sup> Physics Department, University of Florida, Gainesville, FL 32611, USA; buchler@phys.ufl.edu

<sup>2</sup> Research School of Astronomy & Astrophysics, Australian National University, Canberra, AUSTRALIA, wood@mso.anu.edu.au

<sup>3</sup> Warsaw University Observatory, Al. Ujazdowskie 4, 00-478 Warszawa, POLAND, soszynsk@astrouw.edu.pl

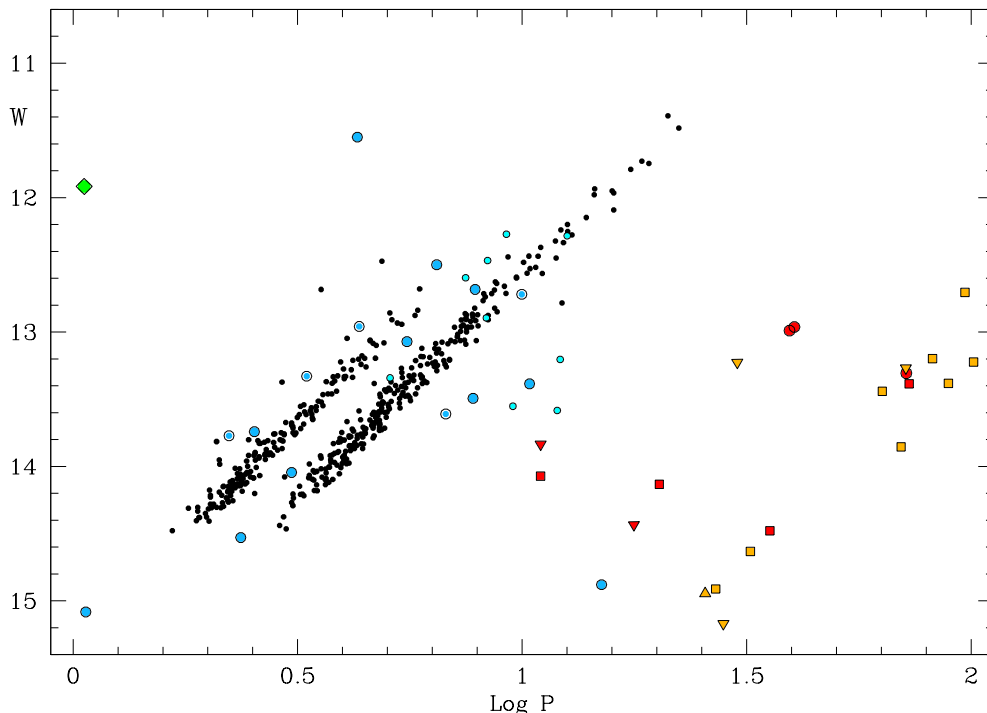


FIG. 1.— Period- $W$  plot for all singly periodic variables of all amplitudes: ULA variables (light blue and cyan), Classical Cepheids (black dots); other larger amplitude objects categorized by light curve shape: non alternating (upside down triangles), regularly alternating (squares), semiregular alternations (circles), ULA alternating (triangle); Pop. II variable stars (red), binaries (orange); special object (green diamond). See text for further details.

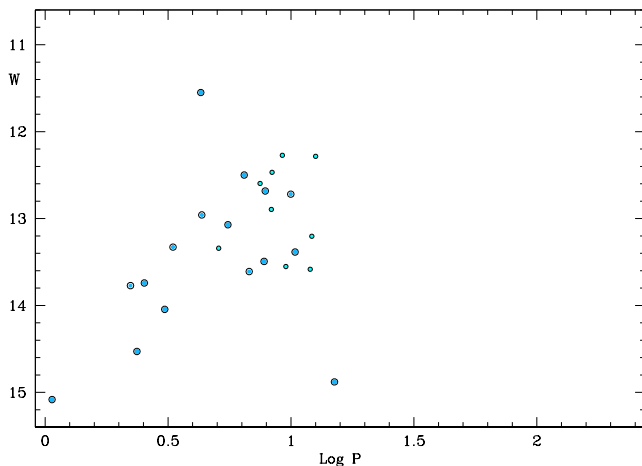


FIG. 2.— Top: Period- $W$  plot of all singly periodic ULA variables in the searched period range, showing a clear clustering in the Cepheid instability strip.

all significant peaks of frequency  $f$  occur with an alias at  $1 - f$ , *i.e.*, with peaks placed symmetrically around the frequency  $0.5 \text{ d}^{-1}$ . The peaks can be of comparable amplitude. The ambiguity of the period determination can generally be resolved by a comparison of the peaks in  $M_R$ ,  $M_B$ , OGLE I and V. When the symmetrically placed peak is absent, which happens when the original peak is barely above the noise, it likely is an indication that the frequency is spurious.

The objects we have found have been grouped into a singly periodic and a multiperiodic set, and will present them separately.

## 2. SINGLY PERIODIC OBJECTS

Figure 1 displays *all the singly periodic* variables that we have uncovered in a period-magnitude (PM) diagram.  $W = I - 1.55(V - I)$  is the Wesenheit function, a reddening-free magnitude estimate. We now attempt to identify the nature of these objects.

The black dots in Fig. 1 fall on two parallel bands which correspond to the fundamental and overtone classical Cepheids. They are included in the figures for reference purposes. All these Cepheids have I band amplitudes greater than  $\sim 0.015 \text{ mag}$ .

The red and orange symbols below the classical Cepheids have relatively large amplitudes. We will return to them below.

The 25 ULA variables we have found are listed in Table 1. All objects have I band amplitudes less than 0.0067, except for SC15 5854 which has an amplitude of 0.0115. The first two columns of Table 1 give the MA-CHO and OGLE names, respectively, followed by the average I magnitude and  $(V-I)$  color, and the period,  $P_R$ , frequency  $f_R$ , and the Fourier amplitudes in  $M_R$  and in OGLE I. The frequency  $f_R$  (and period) is optimized in a linear squares Fourier fit to the  $M_R$  data starting with the highest  $M_R$  spectral peak.

The penultimate column denotes the bands in which there is a strong common peak in the Fourier spectra. By strong we mean that its amplitude stands out by at least a factor of two above the noise level. The asterisk in the last column denotes stars that were already discussed by Buchler *et al.* (2005).

We have plotted the ULA variables as light blue and cyan circles. For the four ULA objects that are branded

TABLE 1  
SINGLY PERIODIC ULA OBJECTS

Columns: OGLE and MACHO IDs, I band mag, color, period, frequency,  $M_R$  and OGLE I band Fourier amplitudes. See text for cols. 9 and 10. Object SC2 357794 lies considerably above the Cepheid P–M relation ( $W$ ,  $\text{Log } P$ ) and is a strange Cepheid candidate.

OGLE	MACHO	I	(V-I)	$P_R$	$f_R$	$A_R$	$A_I$		
SC6 57397	78.6463.64	15.220	0.444	2.3629	0.42320	0.0102	0.0091	RBI	
SC8 76141	79.5746.15	13.994	0.846	7.8600	0.12723	0.0090	0.0057	RBI	
SC11 325504	79.4779.17	13.772	0.821	6.4537	0.15495	0.0027	0.0028	RBI	
SC15 5854	17.3199.23	15.496	0.267	1.0674	0.93685	0.0080	0.0115	RBI	
SC13 223889	1.4295.12	14.452	0.891	5.5415	0.18046	0.0030	0.0039	RBI	
SC1 335392	81.8881.40	14.679	0.835	10.3895	0.09625	0.0036	0.0028	RBI	
SC1 330647	81.8758.16	15.307	0.276	15.029	0.06654	0.0036	0.0030	RBI	
SC13 178852	19.4299.298	14.896	0.745	2.5337	0.39467	0.0027	0.0038	RI	x
SC5 416555	77.7189.9	14.161	0.431	7.7750	0.12862	0.0026	0.0019	RI	x
SC15 196983	1.3568.30	14.855	0.523	3.0663	0.32613	0.0029	0.0016	BI	x
SC2 6920	7.8026.17	13.946	0.871	7.4876	0.13355	0.0042	0.0035	RBI	†
SC19 64022	12.10317.10	13.783	0.975	9.2242	0.10841	0.0033	0.0043	RBI	†
SC9 127569	79.5378.48	14.818	0.817	9.5378	0.10485	0.0035	0.0029	RBI	†
SC11 300879	79.4775.9	13.654	0.884	12.600	0.07937	0.0063	0.0067	RBI	†
SC14 7197	1.3561.6	14.580	0.799	5.0807	0.19682	0.0048	0.0045	RBI	†
SC7 344553	80.6351.14	13.886	0.915	8.3764	0.11938	0.0049	0.0025	RBI	†
SC20 181340	12.10922.11	14.873	0.832	11.970	0.08354	0.0049	0.0040	RBI	†
SC21 140323	6.6697.11	14.136	0.801	8.3250	0.12012	0.0041	0.0030	RBI	†
SC13 191166	19.4302.323	14.450	0.804	12.1561	0.08226	0.0032	0.0029	RBI	x†
SC2 357794	81.8392.8	13.109	1.006	4.2964	0.23275	0.0059	0.0013	S RBI	
SC4 296029	77.7428.36	14.819	0.676	2.2250	0.44953	0.0024	0.0022	RBI	*
SC4 323401	77.7430.18	14.505	0.759	3.3116	0.30187	0.0042	0.0033	RI	*
SC3 153959	77.7789.25	14.116	0.901	9.9817	0.10018	0.0045	0.0034	RBI	*
SC3 35239	77.7668.981	14.149	0.768	4.3373	0.23056	0.0054	0.0032	RI	*
SC4 176301	77.7306.43	14.566	0.617	6.7609	0.14791	0.0109	0.0025	RBI	*

with an X, the evidence for very low amplitude periodicity is a little less strong in the sense that it does not satisfy all our criteria. We will return to them shortly.

Because of the observational noise we have no way of distinguishing ULA pulsating stars from ellipsoidal variables. However, we shall argue that there are very few ellipsoids in our sample. For that purpose we present Figure 2 which locates, unencumbered, *only* the ULA variables in the whole range we have analyzed, namely the  $W$  range corresponding to the chosen parallelogram in the HR diagram (see §1) and the frequency range from 0.004 to 0.99 d<sup>-1</sup>, *i.e.*,  $\text{Log } P[\text{d}] = 0.0044 - 2.40$ . The way the ULA objects cluster near the instability strip in the PM diagram suggests that a large majority of the objects are intrinsic variables and are associated with either the classical Cepheids or, the lower lying ones, the Pop. II Cepheids.

In the OGLE data (Udalski et al 2008) each frame was processed with the DoPhot photometry program. In this way independent PSF profile photometry of each object was derived, supplemented with astrometric information (current X, Y position) obtained via PSF fitting. As a result proper motions can be inferred. In fact, unpublished OGLE-III data suggests that 9 objects show proper motion, which in turn suggests that they are foreground stars. They are represented as smaller cyan filled circles in Figs. 1 and 2, and are branded with a dagger in column 10 of Table 1. However, if they are indeed foreground stars in the solar vicinity that overlap in the CMD with

the LMC instability strip (Soszyński *et al.* 2002) it is nevertheless curious that 6 of them, additionally, appear so near the LMC classical Cepheid PM relations, and the other 3 cluster just below.

If they are foreground stars, one would think that they are some sort of main-sequence ellipsoidal binary in the solar vicinity. Generally, spectra can be used to tell giants from dwarfs and to derive radial velocities, so potentially foreground or LMC status could be investigated by spectral observations, along with radial velocity variations to check binarity *vs.* pulsation.

For completeness, we note that we have also found one egregious large amplitude variable in the database, *viz.* SC8 81586 (79.5626.10). Despite the relative sparsity of its OGLE and MACHO data and the noisiness of its MACHO data this object has a sharply defined period of  $P = 1.0589$  d, and relatively large amplitudes ( $A_R = 0.024$ ,  $A_I = 0.025$ ,  $A_B = 0.036$ ). It is depicted as a green diamond in the upper left side in Fig. 1.

### 2.1. Fourier Spectra and Light Curves of the Singly Periodic Ultra-low Amplitude (ULA) Objects

Plots of the results of our Fourier analysis of each of these objects would take up too much space in this paper. We therefore give just a few representative examples.

Our figures are in a standard format and contain: (1) Panels with the amplitude Fourier spectra for the  $M_R$ ,  $M_B$  and OGLE I, respectively, plotted for a frequency range of 0.004 to 0.99 d<sup>-1</sup>. (2) Panels with the actual data points on the bottom right; because the OGLE ob-

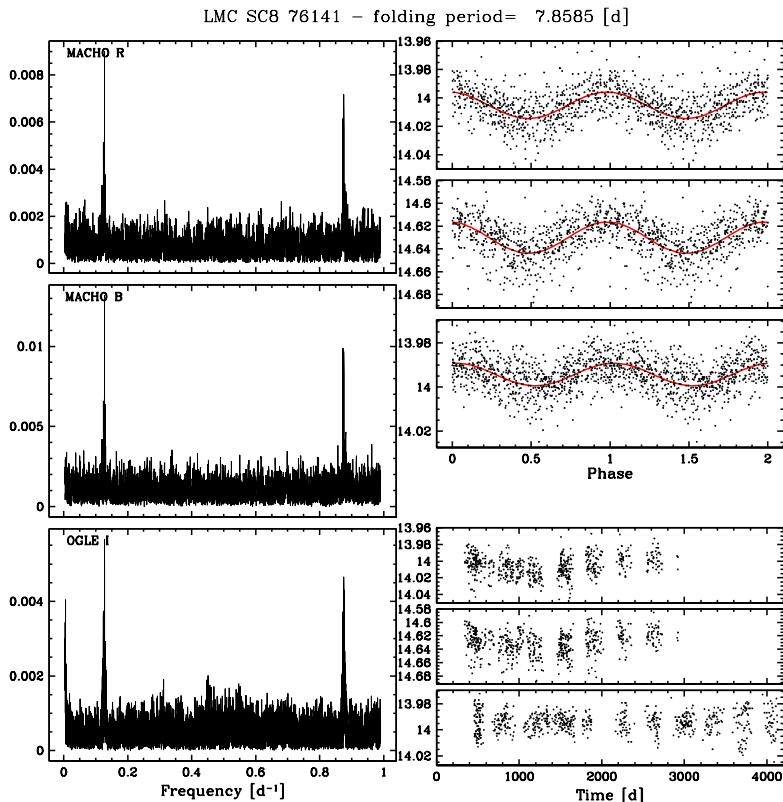


FIG. 3.— LMC SC8 76141 – Left side, top down: Fourier amplitude spectra of the  $M_R$ ,  $M_B$  and OGLE I data; Right side, top: folded and phased data; folding period appears on top; bottom: corresponding data points.

servations start three and 3/4 years (1376.5 days) after the MACHO observations we have shifted them backwards in time in the OGLE panel for better visualization. (3) Panels on the top right side that display the light curves folded with the period that is indicated on top of the figure; the MACHO and OGLE data have been phased by taking the 1376.5d shift into account. The solid red curves in the top right panels represent single frequency harmonic fits to the phased and folded  $M_R$ ,  $M_B$ , and OGLE I data. In some cases we have made small adjustments to the folding period  $f_R$  to improve the phasing.

The analyses of SC8 76141, SC14 7197, and SC11 325504 are exhibited in Figs. 3 – 5. They are among the top 16 objects of Table 1 and they satisfy all our criteria for variability, *viz.* clear peaks in all 3 bands, a strong 1 day alias, good consistent phasing of the folded light curves.

Finally, we wish to give two examples of variability at the confidence limit. Fig. 6 displays the analysis of SC13 178852. The OGLE I data have a very convincing spectrum with a dominant peak at  $0.3947\text{d}^{-1}$ . While the corresponding peak is indeed the largest in  $M_R$  and  $M_B$ , one would perhaps not have claimed variability on the basis of the MACHO or the OGLE data alone. However, it is unlikely that the *same* object would show common peaks, however weak if the variability were not real. Note also that the  $M_R$  spectrum shows the 1-f alias and that there is a strong hint of it in the OGLE I spectrum. Furthermore, the folded light curves show in-phase variability.

In Fig. 7 we present perhaps our weakest case (SC15 196983) for variability. OGLE I and  $M_B$  have their dominant peak at  $f_0 = 0.3261\text{d}^{-1}$ . OGLE I has a strong 1 day alias peak at 0.6739, which is also present in  $M_B$  albeit just barely. However this is the prominent peak in  $M_R$  where the  $f_0$  peak is hidden in the ‘grass’. We have chosen the  $f_0$  peak as the actual frequency of this object for two reasons: first because it is the dominant peak in the OGLE I data which have the cleanest spectrum, and second, because the other peak gives a bad phasing between the folded MACHO and OGLE data.

## 2.2. Discussion

Since many of the objects lie in crowded fields the question arises as to the reliability of our assignments. The variability analysis and the periods that have been determined are immune to contamination by neighboring objects unless those objects have variability themselves or our object is part of a binary, for example.

On the other hand, contamination by a neighboring object will affect the magnitude and the color of our objects. We have looked in some detail at the 3 objects SC4 62503, SC5 124597 and SC4 295930, for example. The first two are isolated objects, but the third one is a messy clump, so it is possible (but not necessary) that the photometry of this last object is poor. This will apply to both the OGLE and MACHO data. V-I for this object is 1.38, way outside the typical range (see the CM plot of Fig 8. A further look at SC4 295930 in I- $M_R$ , V- $M_B$  and V-I reveals that I is anomalously bright, by at least 0.5 mag. Consequently, it should be shifted down in the PM plot and could well be a regular classical Cepheid

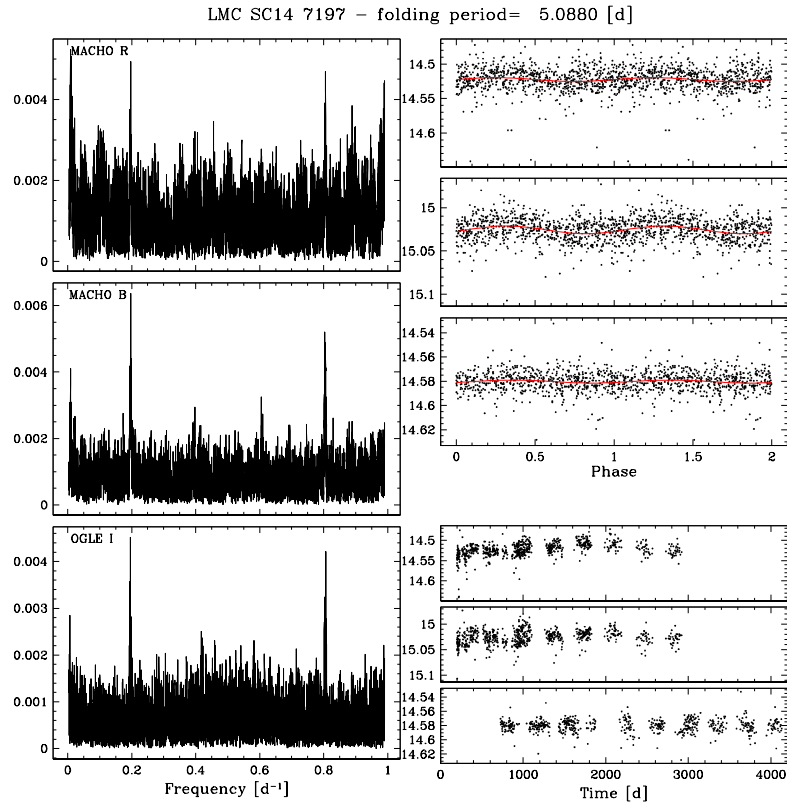


FIG. 4.— LMC SC14 7197 – Left side, top down: Fourier amplitude spectra of the  $M_R$ ,  $M_B$  and OGLE I data; Right side, top: folded and phased data; folding period appears on top; bottom: corresponding data points.

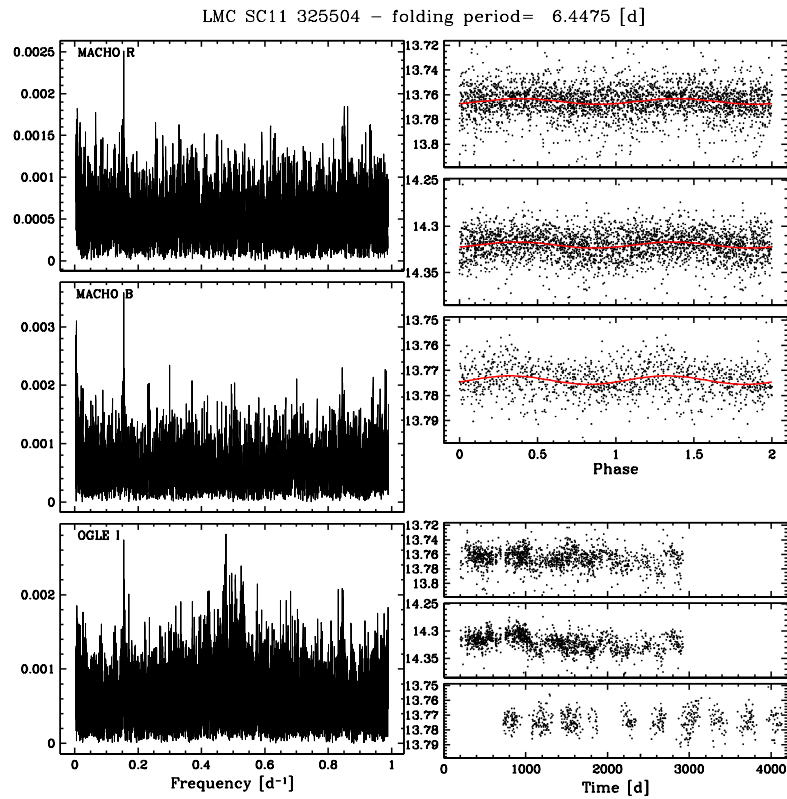


FIG. 5.— LMC SC11 325504 – Left side, top down: Fourier amplitude spectra of the  $M_R$ ,  $M_B$  and OGLE I data; Right side, top: folded and phased data; folding period appears on top; bottom: corresponding data points.

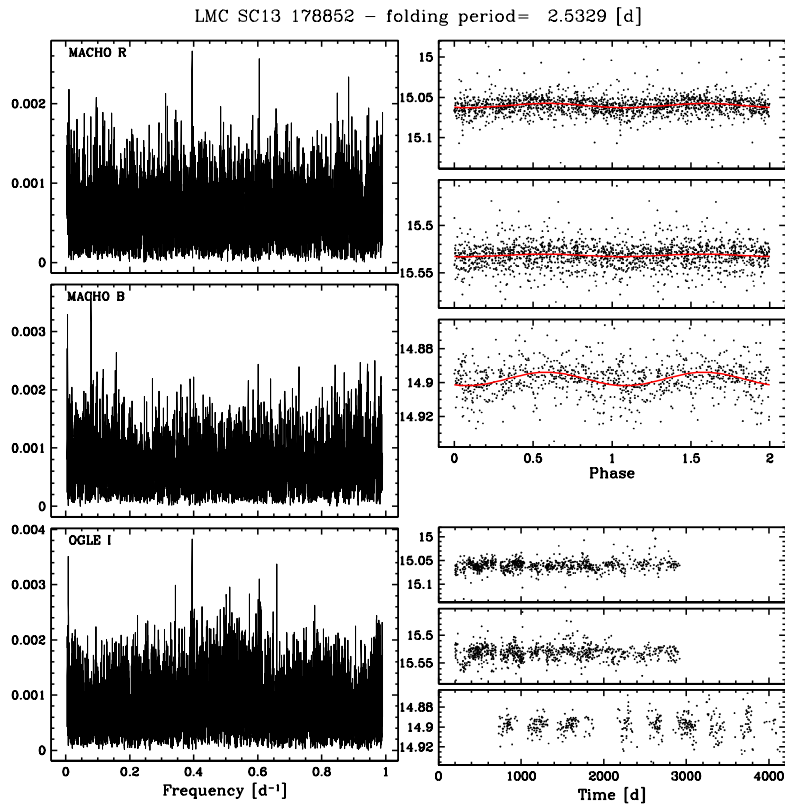


FIG. 6.— LMC SC13 178852 – Left side, top down: Fourier amplitude spectra of the  $M_R$ ,  $M_B$  and OGLE I data; Right side, top: folded and phased data; folding period appears on top; bottom: corresponding data points.

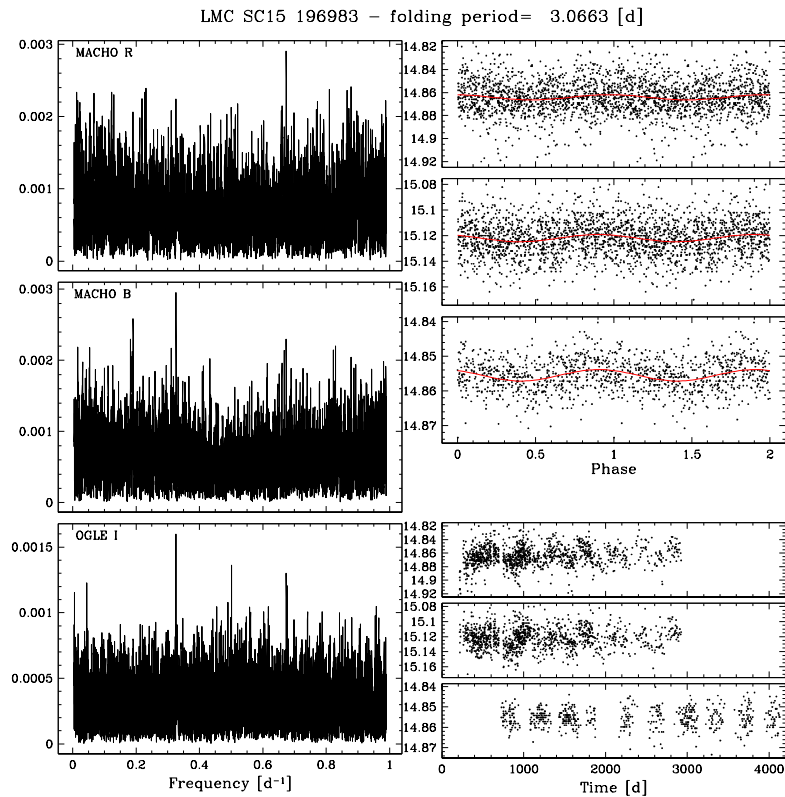


FIG. 7.— LMC SC15 196983 – Left side, top down: Fourier amplitude spectra of the  $M_R$ ,  $M_B$  and OGLE I data; Right side, top: folded and phased data; folding period appears on top; bottom: corresponding data points.

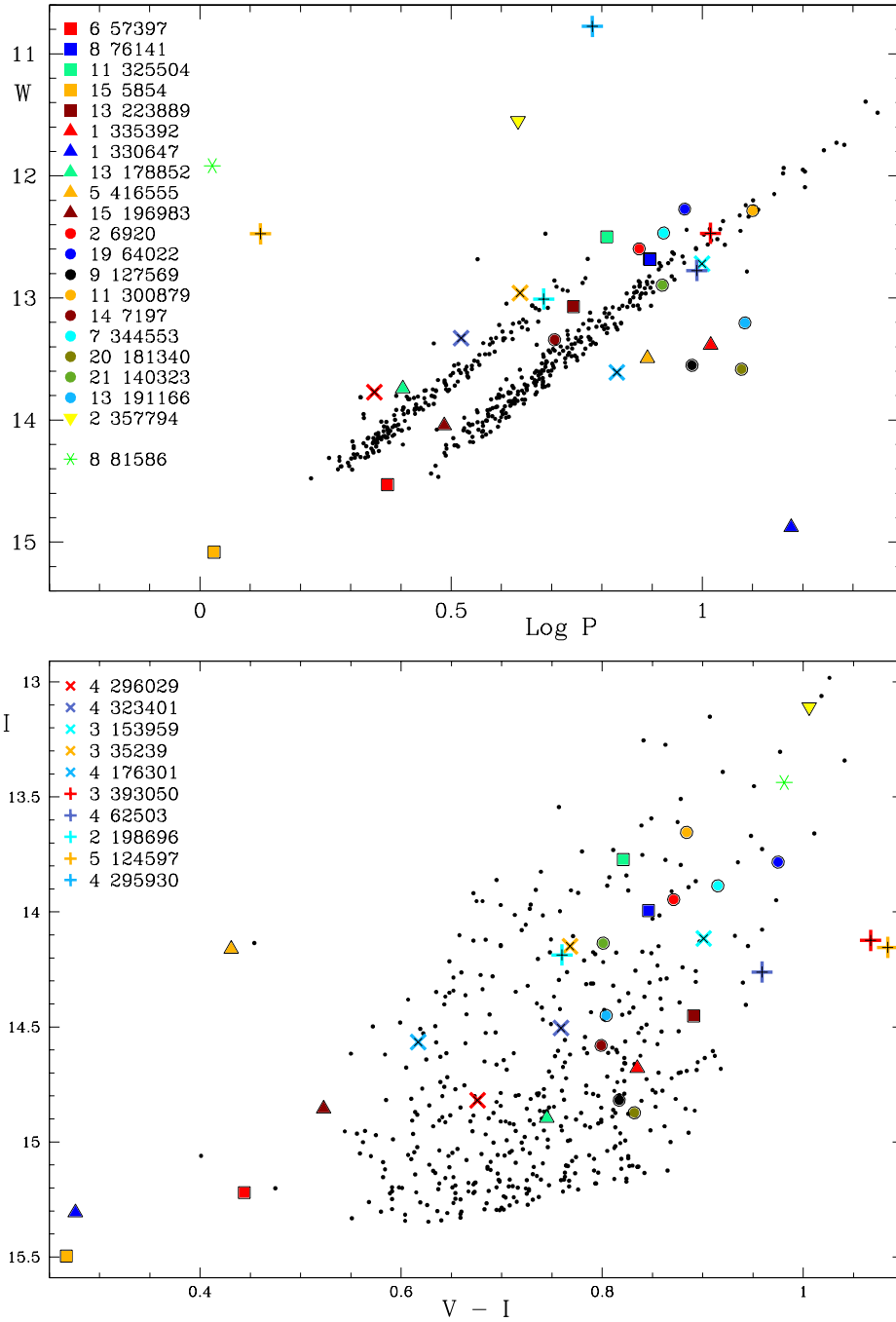


FIG. 8.— Top: Period- $W$  plot for ULA variables (large symbols), where  $W = I - 1.55(V - I)$ . Also shown are the classical Cepheids (small black dots) from our combined MACHO-OGLE data base. Bottom:  $I, V-I$  plot for the same stars. The black dots represent the classical Cepheids. The 5 squares, 5 triangles and 9 filled circles mark the position of the ULA Cepheids, the upside-down triangle that of the potential strange Cepheid candidate SC2 357794. The crosses and Xs denote the objects from Buchler *et al.* (2005). SC4 295930 has a  $V-I = 1.38$ , outside the plotted range. The green asterisk in the color-magnitude diagram locates the egregious variable star SC8 81585 that is located in the upper left corner in Fig. 1.

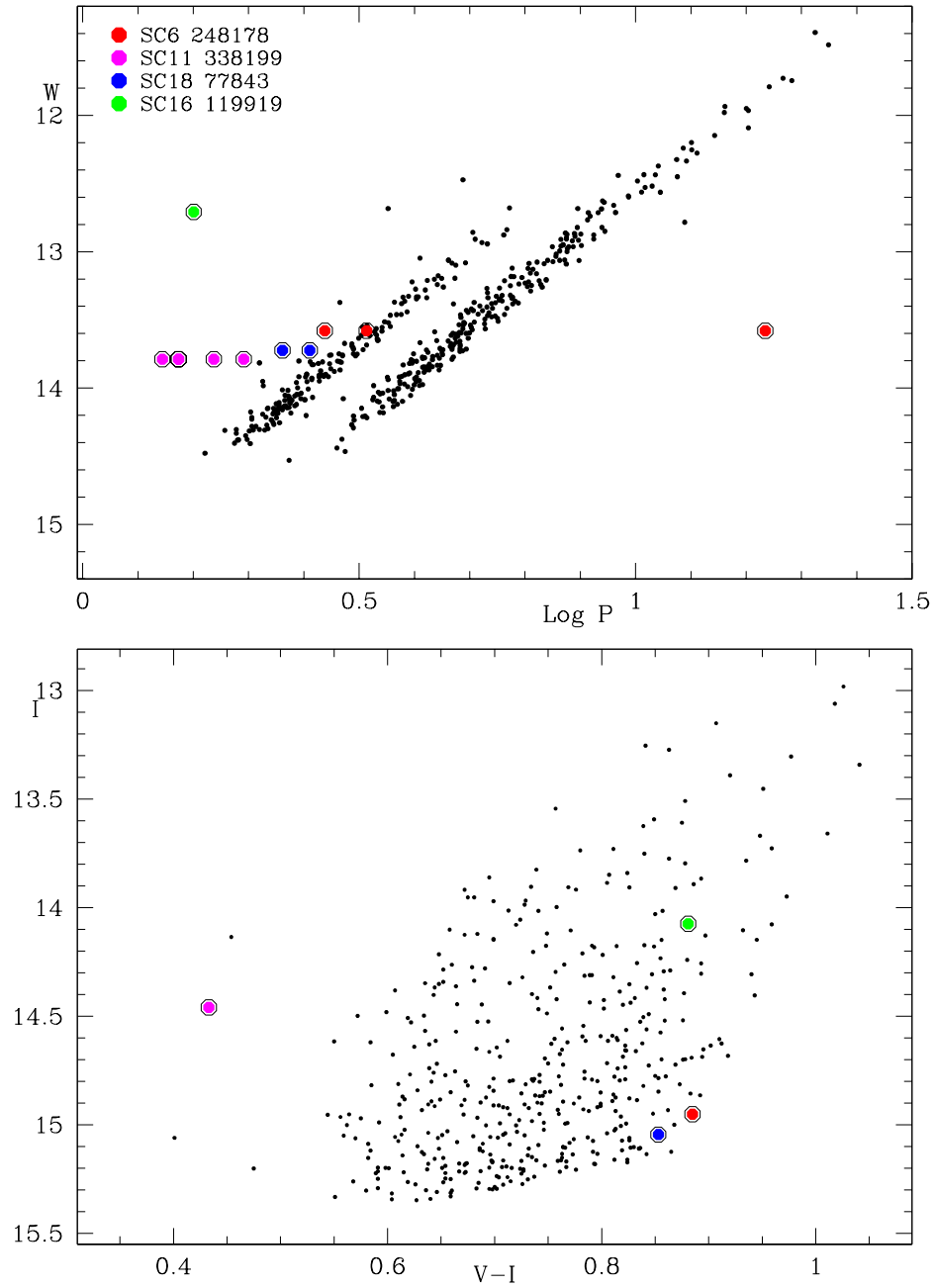


FIG. 9.— Top: Period- $W$  magnitude plot. The objects of this paper are superposed on the Cepheids from our combined MACHO-OGLE data base. The various periods of each star appear on a horizontal alignment; Bottom:  $(I, V-I)$  CM plot.



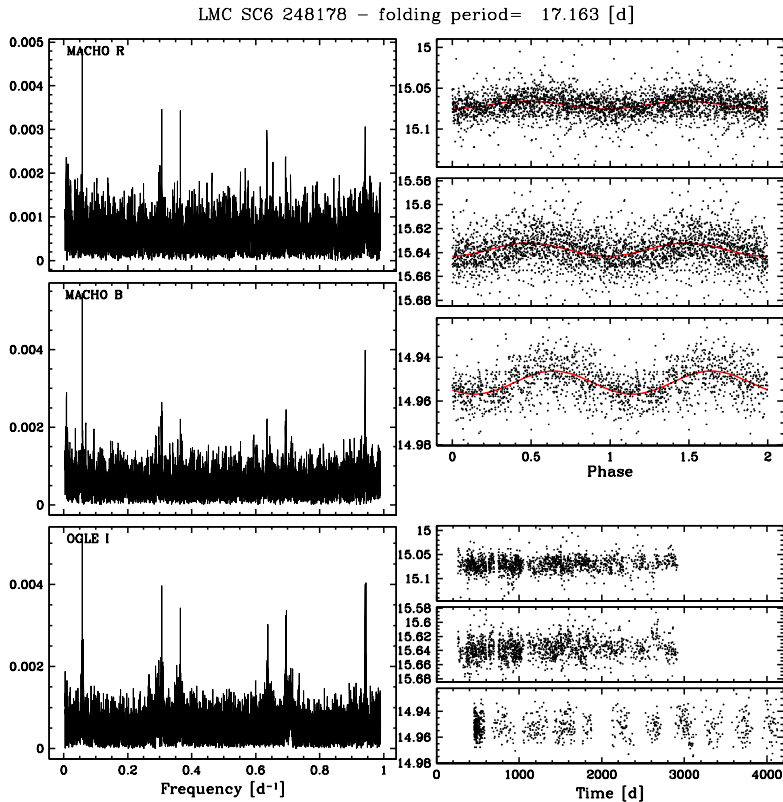


FIG. 10.— LMC SC6 248178 – Left side, top down: Fourier amplitude spectra of the  $M_R$ ,  $M_B$  and OGLE I data; Right side, top: folded and phased data; folding period appears on top; bottom: corresponding data points.

of very low amplitude rather than a strange Cepheid.

We now turn to Fig. 8. The top panel is a blowup of the PM ( $\log P$ ,  $W$ ) plot of Fig. 1, and the bottom panel is the corresponding CM ( $V-I$ ,  $I$ ) plot. All the objects that are listed in Table 1 and in Buchler *et al.* (2005) are identifiable in the figure. The squares, diamonds, filled circles and upright triangles indicate the newly found ULAs. The filled circles locate the potential foreground objects. The Xs denote the 5 variables that are in common with the previous work of Buchler *et al.* (2005) which concentrated on MACHO Field 77. The crosses are their additional variables that lie marginally outside the cut that defines this paper’s data base (see §1). For reference we have again plotted the classical Cepheids as small black dots.

These ULA objects are certainly a mixture of pulsating stars with perhaps a few ellipsoidal that can also have amplitudes in the millimag range. Of course, the ULA Cepheids have to satisfy the known PM relations, but it is difficult to distinguish between these two types of low amplitude variability.

One notes that 20 objects of Table 1 fall into the classical Cepheid range, in both the PM and the CM diagrams. Most of the ULA objects fall outside of or near the edges of the F and O1 instability strips. That ULA Cepheids would be at the edges of the instability strip is consistent with theory (Buchler & Kollath 2002; Buchler *et al.* 2005).

However one might claim that the figure indicates that the ULA objects form two separate, parallel fundamental and overtone PM relations in which case they would be

physically distinct from the regular Cepheids (perhaps on the first crossing of the instability strip rather than on the second or third crossings on the blue loop). The color-magnitude diagram, unfortunately has too much scatter to provide any discriminating information.

One object, SC15 5854, with a period of 1.0674 d lies in the continuation of the Cepheid PM relation and falls into the CM range of the Cepheids, albeit quite beyond the tip.

There is a cluster of 6 stars that falls below the Cepheid PM relation with periods 2–3 times longer than that of classical Cepheids of the same magnitude. Three of them are possibly foreground stars, as discussed in §2. Again, we cannot be sure that these objects are not ellipsoidal, but it seems unlikely because of the clustering in PM. Furthermore, 4 of them (SC9 127569, SC20 181340, SC1 335382, and SC13 191166) also cluster in CM. This suggests that they are pulsators rather than ellipsoidal. What is their nature? They are unlikely to be classical Cepheids because they have too small a brightness for their period, and potential contamination by neighboring objects would move them even lower in the PM diagram. It is possible that these stars are also ULA Population II stars. However, SC5 416555, which is very blue is perhaps an ellipsoidal.

The star SC2 357794, marked with an inverted triangle in Fig. 8, falls into the proper CM range, but it has a period a factor of  $\sim 5$  smaller than the fundamental Cepheid period, *i.e.*, the period the star would have if it pulsated in the F mode. The theoretical work of Buchler *et al.* (1997) has shown that some Cepheids

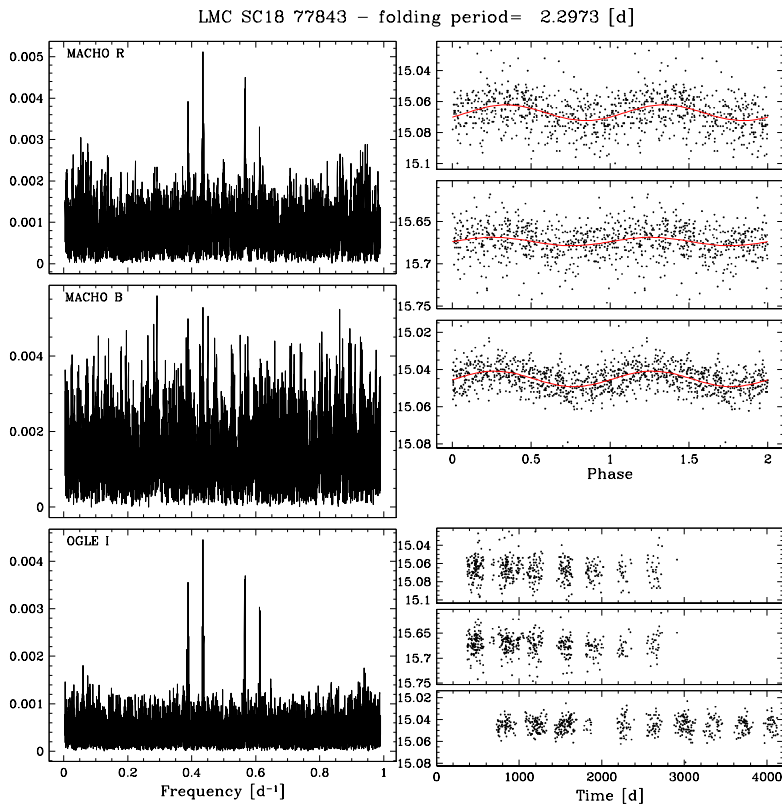


FIG. 11.— LMC SC18 77843 – Left side, top down: Fourier amplitude spectra of the  $M_R$ ,  $M_B$  and OGLE I data; Right side, top: folded and phased data; folding period appears on top; bottom: corresponding data points.

can pulsate in a surface mode with a period that is about a factor of 4–5 shorter than the corresponding fundamental period. This object therefore is possibly a strange Cepheid (Buchler & Kollath 2001). But one cannot rule out that the light curve might be contaminated by a bright nearby star in which case it could be a regular ULA Cepheid as we already suggested for object SC5 124597 that Buchler *et al.* (2005) had identified as a strange Cepheid candidate.

Object SC1 330647 is a little offset with  $W \sim 15$  and  $\text{Log } P \sim 1.2$  and lies in the W Vir instability region (see Fig. 1). It could be a ULA W Vir star although its V–I color is very blue.

We conclude that most if not all of the ULA singly periodic objects in the data set are Pop. I and Pop. II Cepheids, with the caveat that some might be foreground stars or ellipsoidal.

### 2.3. Other, Larger Amplitude Variable Objects

We now turn to the larger amplitude singly periodic stars that are exhibited in Table 2. The objects that we identify as probable binaries are marked in orange and the probable Pop. II or RV Tau in red in Fig. 1.

Their identifiers, their average I magnitudes, Wesenheit magnitudes  $W$  and their periods (or cycling times) are given in Table 2. The first two columns give the MACHO and OGLE names. All these stars have I band Fourier amplitudes in the range 0.01 to 0.25. An exception is the ULA SC3 201554 with harmonic peak amplitudes of 0.0065 and 0.0075, that is shown in yellow. The objects that are displayed as triangles have regular light curves. One object, SC4 53483, has a ‘crested top’

light curve that is typical of some W Vir stars. The remainder show behavior with cycle to cycle alternations. These alternations are regular (squares) for some and some semi-regular (circles).

The period association is sometimes ambiguous by a factor of 2 when alternations are present. We have not chosen the period with the highest Fourier peak, but somewhat arbitrarily the one that gives visually the folded light curve with the least scatter.

One notes that all but 2 points would fall on 2 parallel, relatively tight PM relations that are separated by 0.3 (factor of 2 in  $P$ ). The binaries (orange) fall predominantly on the right sequence, and the Pop. II/RV tau stars (red) predominantly on the left one.

Actually, from a physical point of view, for the pulsating stars the shorter period is more relevant as it corresponds to the linearly excited pulsational mode, whereas the longer period arises through period doubling that is caused by nonlinear effects (Buchler & Kovacs (1986), Kovacs & Buchler (1987)).

For the binaries, the reverse situation holds. Here there are also two sequences separated by 0.3 in  $\text{Log } P$  because the “no alt” stars can adopt a period equal to half the orbital period (there are two maxima per orbit).

But, why does the binary sequence exist? We will argue that it is because stars on the blue loops have a certain size at a given luminosity and color, and if they have a companion that is capable of causing ellipsoidal variations, it must be at a small multiple of the stellar radius. This radius increases with luminosity (I) and color (V–I). The conversion to  $W$  will tend to take out the V–I variation along tracks at given luminosity. If we remember

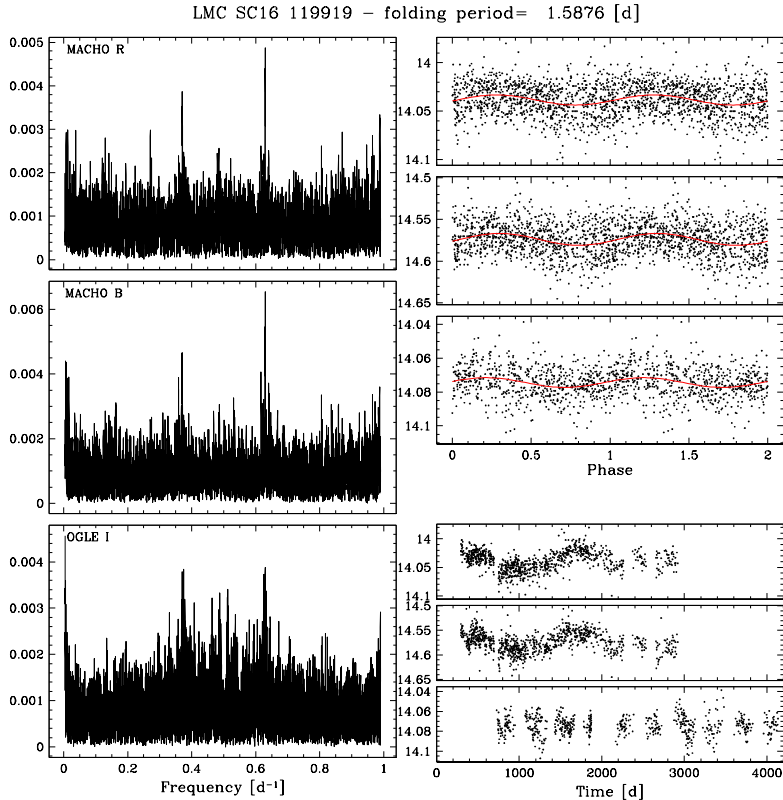


FIG. 12.— LMC SC16 119919 – Left side, top down: Fourier amplitude spectra of the  $M_R$ ,  $M_B$  and OGLE I data; Right side, top: folded and phased data; folding period appears on top; bottom: corresponding data points.

that for both orbits and pulsation,  $P \sim R^{1.5}$ , and that the period of the fundamental pulsation mode is not too different from the orbital period at the stellar surface, we can see that qualitatively the binary sequence should be parallel to the pulsation sequence: more detailed computations would be needed to estimate the exact shift in  $\log P$ . The stars on the binary sequence should therefore be in the LMC.

We have found low amplitude RV Tauri and Pop. II Cepheids in the LMC that do not appear in the catalogs of (Alcock et al. 1999; Udalski et al 1999). We also find that, curiously, a set of binaries appear to lie on essentially the same PM relation as the RV Tauri/Pop. II Cepheids.

### 3. MULTIPERIODIC VARIABLES

Four of the ULA stars have multiple periods. They are displayed in the PM plot of Fig. 9. Again for reference we have superposed the Cepheids as small black dots. The bottom panel displays the corresponding (I, V-I) plot. The properties of these objects appear in Table 3.

The results of the individual Fourier analyses are presented in Figs. (10, 11, 12 and 13).

\* LMC SC6 248178: The results of the analysis are displayed in Fig. 10. Table 3 indicates that this star has its largest frequency peak at  $f_1 = 0.05819 \text{ d}^{-1}$ , *i.e.*, 17.185 d, and two close frequencies,  $f_2 = 0.36484$  and  $f_3 = 0.30657 \text{ d}^{-1}$ . One notes that  $f_3 \sim f_2 + f_1$ . Even though the 3 amplitudes are all in the low millimag range, the 3 peaks stand out very clearly in  $M_R$ ,  $M_B$  and OGLE I. Peaks 2 and 3 suggest that if this star is a Cepheid it

may be a higher order double-mode pulsator with a large period ratio of  $P_3/P_2 = 0.84028$ . If the long period of 17.185 d were due to an unseen binary companion that would not explain the observed frequency lock.

\* LMC SC18 77843: The analysis of this object appears in Fig. 11. There are two peaks with a period ratio of 0.89177 which is larger than that of a double mode Cepheid that pulsates in the O1 and O2 modes. The star also lies somewhat to the left of the PM relation, both when plotted with I and with the Wesenheit magnitude  $W$ , consistent with the expected positions of higher order modes.

\* LMC SC16 119919: This star is a 1.59 d period variable with an extremely long period (1380 d) modulation (Fig. 12). Looking at the light curve points one would think that we have mismatched the OGLE object with the wrong MACHO object. However the spectral peaks and the phased, folded light curves suggest otherwise.

The 1.59 d period is much shorter than expected for a Cepheid of similar magnitude and color. Similarly, the long 1380 d is hard to explain. It could be a binary with a very bright companion, although the amplitude of the long period variation would be very large for ellipsoidal motion. The period ratio is also at odds with that of the blue multi periodic variables that Mennickent *et al.* (2003) discovered.

\* LMC SC11 338199: This star is multiperiodic with 4 frequencies that show up simultaneously in  $M_R$ ,  $M_B$  and OGLE I (Fig. 13). No other peaks seem to be significant. All four periods are consistent with low order

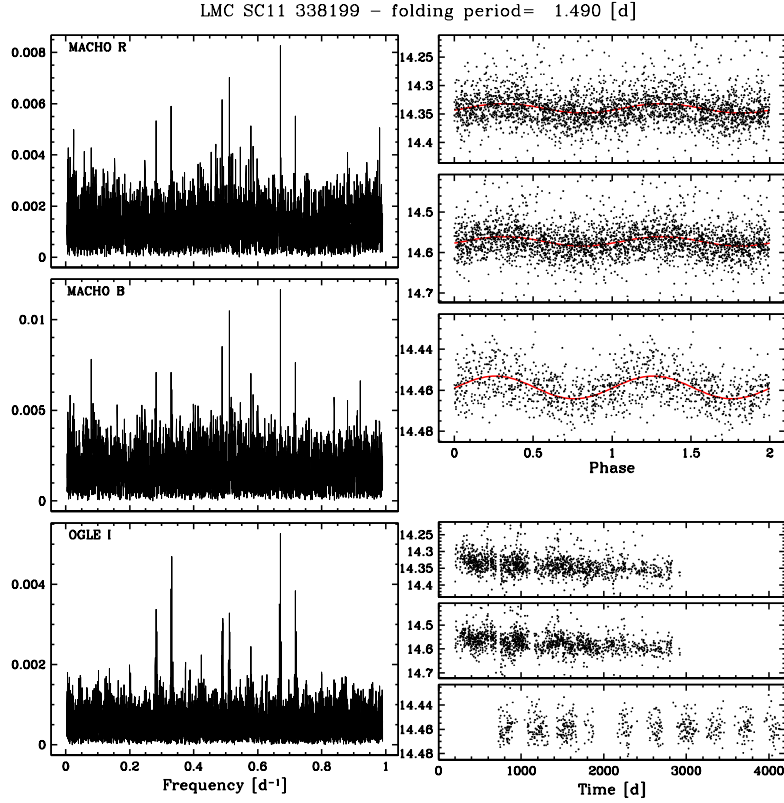


FIG. 13.— LMC SC11 338199 – Left side, top down: Fourier amplitude spectra of the  $M_R$ ,  $M_B$  and OGLE I data; Right side, top: folded and phased data; folding period appears on top; bottom: corresponding data points.

TABLE 2  
LARGER AMPLITUDE SINGLY PERIODIC OBJECTS

Columns: OGLE and MACHO IDs, I band mag, period, I band Fourier amplitude, star type. In the case of alternating cycles, the period has been chosen to visually give the best folded light curve, rather than to correspond to the Fourier peak with the highest amplitude.

OGLE ID	MACHO ID	$M_I$	$W$	P[d]	$A_I$		Type of star
SC21 85305	6.6575.25	15.065	14.071	10.99		alt	Pop. II
SC8 52612	79.5622.20	14.638	13.835	10.99	0.038	no alt	Pop. II
SC7 295173	78.6223.44	15.036	14.435	17.74	0.037	no alt	Pop. II
SC4 53483	77.7306.73	14.902	14.133	20.21		crested	Pop. II
SC4 287444	77.7426.59	15.288	14.911	26.97		alt	binary
SC1 325044	81.8758.27	15.533	15.170	28.06	0.015	no alt	binary
SC6 462158	80.6710.17	14.113	13.226	30.14	0.014	no alt	binary
SC10 137113	2.4902.4632	15.175	14.633	32.22		alt	
SC10 105184	79.4896.51	15.225	14.478	35.61		alt	Pop. II
SC5 92493	78.6949.2259	14.090	12.989	39.4		semireg	Pop. II
SC3 274381	77.7911.4	14.105	12.963	40.4		semireg	Pop. II
SC14 57979	19.3694.19	14.662	13.441	63.40		alt	binary
SC11 338244	79.4659.3417	14.972	13.854	69.82		alt	binary
SC11 338203	79.4780.27	14.569	13.306	71.7		semireg	Pop. II
SC9 263456	79.5504.13	14.684	13.267	71.78	0.057	no alt	binary
SC6 40874	78.6461.2152	14.361	13.385	72.76		alt	Pop. II
SC8 181816	78.5856.2363	14.383	13.197	81.99		alt	binary
SC14 100796	1.3810.19	14.038	13.382	88.95		alt	binary
SC9 237168	79.5501.13	13.845	12.706	96.90		alt	binary
SC14 100798	1.3810.30	14.323	13.226	101.26		alt	binary
SC3 201554	77.7794.46	15.527	14.9457	25.57	0.007	binary	

TABLE 3  
ULA MULTIMODE STARS

Columns: OGLE and MACHO identifiers, I magnitude, V-I color, significant frequencies, corresponding  $M_R$  Fourier amplitudes. (The last object's amplitude is a little larger than our ULA criterion). A dagger in the last column denotes potential proper motion.

OGLE	MACHO	I	(V-I)	$f_1$	$f_2$	$f_3$	$f_4$	$A_1$	$A_2$	$A_3$	$A_4$
SC6 248178	78.6699.27	14.951	0.885	0.05819	0.36484	0.30657		0.0048	0.0034	0.0034	
SC18 77843	11.9838.21	15.045	0.853	0.43528	0.38817			0.0050	0.0039		
SC16 119919	81.8998.12	14.074	0.881	0.63018	0.00072			0.0048	0.0159		
SC11 338199	79.4659.3384	14.459	0.433	0.67103	0.51146	0.71783	0.57911	0.0083	0.0070	0.0055	0.0051 †

radial pulsation modes, but it is not obvious why they they should all be excited for a star of this brightness. However, there is always the possibility that the light curves of this object are contaminated by a neighboring star, in which case it would fall into a brightness regime where one might expect AI Velorum type multimode pulsation.

There is recent evidence for proper motion in this star (Udalski et al 2008, unpublished OGLE-III results). If SC11 338199 is a foreground star that would make it even brighter and its nature harder to explain.

#### 4. SUMMARY

Fourier analysis of the light curves of LMC stars in the very broad vicinity of the Cepheid instability strip part yielded 25 new singly periodic and 4 new multiperiodic variables with ultra-low amplitudes (ULA) ( $\lesssim 0.01$  mag). The advantage of our approach has been that, for many of these objects, it would be difficult to claim variability on the basis of either the MACHO or the OGLE data only. In addition, we have found RV Tauri and Pop. II Cepheids that do not appear in either the MACHO or OGLE catalogs.

If we include the objects of Buchler *et al.* (2005) we have 20 ULA objects that fall close to the fundamental (F) and overtone (O) Cepheid PM relations. From Fig. 8 it appears that these stars might form separate sequences that are slightly above and parallel to the classical F and O LMC Cepheids. If this effect turns out to be real it will pose an interesting challenge to explain the nature of

these objects. There is evidence that 9 of these ULA stars show proper motions and that they could be foreground stars, but that raises other questions as to their nature. Even if we accept them as foreground this still leaves enough (14 instead of 20) objects to suggest separate PM relations.

Combining this and previous work (Buchler *et al.* 2005) we now have 3 stars that are strange Cepheid candidates (Buchler & Kollath 2001), although the light curve of one of them, SC4 295930, could be contaminated by a very bright red star which would place it erroneously above the PM relation.

Six closely clustered objects fall below the classical Cepheid PM relation (see Fig. 8). They could be ULA Pop. II Cepheids or ellipsoidals, although 3 of them could be foreground stars. A further, very blue object, SC1 330647, could be a ULA W Vir star. Interestingly, a set of binaries appear to lie on essentially a PM relation parallel to that of the RV Tauri/Pop. II Cepheids. Finally, we have uncovered 4 objects that show multiple modes of ultra-low amplitude.

It is a great pleasure to thank Zoltán Kolláth for providing us with his MUFRAAN software. This work has been supported by NSF (AST07-07972 and OISE04-17772) at UF. JRB gratefully acknowledges the hospitality of Mount Stromly Observatory where this work was started. We wish to thank an anonymous referee for his comments which led to a much improved paper.

#### REFERENCES

- Alcock, C. and the MACHO Consortium 1999, PASP 111, 1539  
 Beaulieu, J.P., Grison, P. *et al.* 1995 AA 303, 137  
 Buchler, J.R., Wood, P.R., Keller, S. & Soszynski, I. 2005, ApJ631, L151.  
 Buchler, J. R. & Kolláth, Z., 2001, ApJ255, 961  
 Buchler, J. R. & Kollath, Z 2002, ApJ573, 324.  
 Buchler, J. R. & Kovács, G. 1987, ApJ320, L57  
 Buchler, J.R., Yecko, P.E. & Kolláth, Z. 1997, AA 326, 669  
 Kanbur, S. M., Ngeow *et al.* 2003, AA 411, 361.  
 Kolláth, Z. 1990, *The program package MUFRAAN*, Konkoly Observatory Occasional Technical Notes No. 1  
 Kovács, G. & Buchler, J. R. 1987, ApJ334, 971  
 Mennickent, R.E., Pietrzynski, G., Diaz, M, Gieren, W. 2003, A&A399, L47  
 Soszyński et al., Acta Astr. 52, 143  
 Stellingwerf, R.F. 1978, ApJ, 224, 953  
 Udalski A., *et al.* 1999, Acta Astr. 49, 223  
 Udalski A., *et al.* 2008, Acta Astr. 58, 69  
 Welch, D.L. *et al.* 1995, in “Astrophysical Applications of Stellar Pulsation”, Eds. R.S. Stobie & P.A. Whitelock, ASP Conf. Ser. 83, 232